# The Thermal Behavior of a Developed Zero-cement Backfill in a Novel Technique Used in Arctic Mining

Fatemeh Tavanaei[1], Mehrdad Fadaei Kermani[1], Gongda Lu[2], Agus Sasmito[1], Alessandro Navarra[1], Ferri Hassani[1]

[1] Department of Mining Engineering, Faculty of Engineering, McGill University
[2] Department of Civil Engineering, Faculty of Engineering, McGill University

## Abstract
Mineral resource depletion drives the need for mining in increasingly remote areas using novel methods. Severe conditions in these remote areas can include permafrost. The Chidliak diamond mine of DeBeers, situated in the Arctic Circle, is one such operation. There are many challenges to Arctic mining projects, such as transportation limitations and severe climate conditions. Furthermore, the Chidliak mine has been planned to have the lowest possible carbon footprint. The mining operation applies a novel vertical boring technique from the surface, by which the vertical kimberlite pipe with a diameter of approx 125–150 m and to a depth of 400 m will be excavated. Each boring operation results in a vertical shaft of approx 5 m diameter which is subsequently backfilled. Cement or binder is omitted from the backfill mixture due to transportation cost and adverse effects of low temperature on cementation. Instead, a frozen backfill is employed where water serves as the binder as it freezes. As part of an overall investigation into backfill design, rate of backfill deposition, and mine planning (sequencing of shaft boring and deposition), this paper explores and discusses the thermal behavior and freezing time of the novel backfill technique. The temperature and ice saturation of two filled shafts over time are examined, providing an initial understanding of designing shafts across the entire mine area and optimizing their construction based on climate conditions.

Key words: frozen backfill, Arctic mining, ice saturation, numerical modeling

## Introduction
Depletion of mineral resources is pushing mining operations to more remote areas (Tilton, 2005). However, reaching out to remote areas and converting previously uneconomic resources into valuable reserves requires innovative methods (Seredkin et al., 2016). Employing novel and innovative methods should be assessed using developed tools such as numerical and experimental methods. These innovations should be evaluated in terms of their efficiency and effectiveness as well as their potential impacts on the environment (Booshehrian et al., 2020).

The quantity of mines in northern Canada is consistently rising. For instance, Nunavut has recently gained importance because of its rich mineral potential. Ongoing exploration activities have led to the identification of several mineral deposits, and some of them have already been developed into mines (Bowes-Lyon et al., 2010). To the west, in Canada's Northwest Territories, many mining companies are showing keen interest in the potential wealth of critical minerals. The demand for lithium, nickel, graphite, and copper has surged significantly to meet the requirements of the rapidly growing electric vehicle and solar power industries (Ed Struzik, 2023).

As mining expands in these areas, knowledge about the specifications of these areas and the required special techniques should be developed. One of the restrictions associated with working in Canada's remote regions is a cold and severe climate, which limits the human resource, material transportation, and some conventional chemical reactions, such as the cementation of cemented backfill (Pan et al., 2022). On the other hand, cemented backfill as one of the essential parts of mining, specifically underground mining (Hassani & Archibald, 1998; Sheshpari, 2015), faces difficulties in cold regions. In Arctic areas, backfill becomes frozen in the permafrost ground because of cold weather, which adversely affects cementation

and hydration reactions (Hou et al., 2020a). While cold weather is not favourable to cementation reaction, it is possible to take advantage of this severe condition to freeze backfill and increase the backfill strength (Cluff & Kazakidis, 2013; Pan et al., 2022). Frozen backfill is a sort of new term in mining backfill and is receiving attention due to its higher strength, lower costs (specifically in the case of omitting cement), and the fact that the mining industry is going to need it more because of the growing mines mine development in Arctic areas (Hou et al., 2020b; Jiang et al., 2017; Tavanaei et al., 2023). Although a number of studies have been carried out on frozen backfill strength (Beya et al., 2019; Christ et al., 2010; Xu et al., 2020; Zhang et al., 2020), its thermal behavior is less studied (Gao et al., 2017; Ghoreishi-Madiseh et al., 2011; He et al., 2022).

As the case study, this article has focused on the Chidliak diamond mine located in northeast of the city of Iqaluit, the capital of Nunavut (population 7740 in 2016 Census). The Chidliak diamond mine is in the Arctic Circle and has a permafrost area of approximately 120 km. This mine is being operated by DeBeers and faces challenges such as severe climate conditions (Fitzgerald et al., 2018) and limited transportation (DeBeers, 2022). To minimize environmental impact, the mine employs a unique vertical boring technique to excavate a kimberlite pipe with a 125–150 m diameter. Each boring operation creates a 5 m diameter vertical shaft, which is subsequently filled. The study's initial focus is designing the backfill, considering both mining and environmental constraints. To address transportation costs and the negative impact of low temperatures on cementation, the backfill mixture excludes cement. Instead, water is employed to work as the binder as it freezes in the permafrost ground. In this paper, a numerical analysis is performed to examine the thermal behaviour of the backfilled shafts, measure the time each shaft needs to freeze, and how the ice saturation evolves.

**Mathematical Model**

A novel multiphysics model is developed in this study to investigate the thermal behaviour of backfill deployed in the novel mining technique. The model is able to assess the temperature of each point and the ice saturation within the backfill (as a two-phase porous material) while considering thermal, hydraulic and mechanical modules. The model is developed by further incorporating the multiphysics effects associated with phase change of water into our previous backfill model (Lu et al., 2020; Tao et al., 2022) established under Biot's theory of classical thermo-poroelasticity. The employed physical parameters in the following calculations are described in Table 1. The soil freezing characteristic curve (Figure 1) is employed for effective water saturation vs temperature.

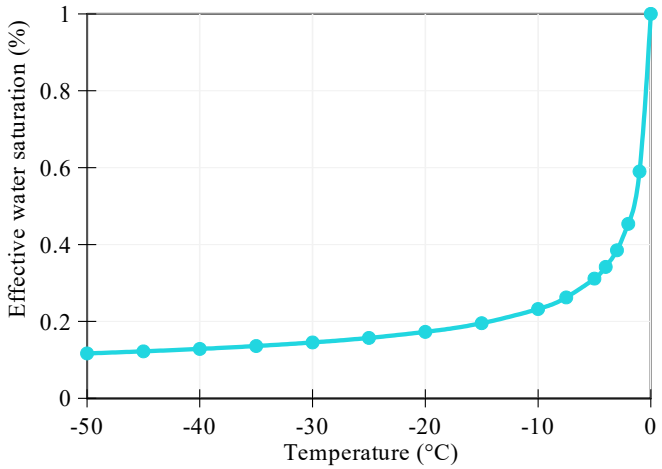


Figure 1. Soil freezing characteristic curve employed for mine backfill.

**Governing equations**

*Energy balance* (Equation 1):

$$[(1-n)\rho_s C_s + nS_w\rho_w C_w + n(1-S_w)\rho_i C_i]\frac{\partial T}{\partial t} + (\rho_w C_w v_{rw})\cdot\nabla T + \nabla\cdot(-k_{eff}\nabla T) = \dot{Q} \quad \text{Equation 1}$$

where subscripts $s$, $w$, and denote solid/rock, water, and ice, respectively, and $n$ is porosity, $\rho$ is density, $C$ is specific heat, $S$ is saturation, $T$ is temperature, $t$ is time, $v_{rw}$ is relative velocity of water, $k_{eff}$ is hydraulic conductivity of backfill, and $Q$ is heat.

*Mass balance* (Equation 2)

The source term for phase change has been cancelled during manipulation:

$$S_w\left(\frac{\alpha-n}{K_s}+\frac{n}{K_w}\right)\frac{Dp_w}{Dt} + (1-S_w)\left(\frac{\alpha-n}{K_s}+\frac{n}{K_i}\right)\frac{Dp_i}{Dt} - \frac{\alpha-n}{K_s}S_{cryo}\frac{DS_w}{Dt}$$
$$-[\beta_s(\alpha-n)+nS_w\beta_w+\beta_i n(1-S_w)]\frac{DT}{Dt} + \frac{1}{\rho_w}\nabla\cdot(nS\rho_w v_{ws}) + \alpha\frac{\partial\varepsilon_v}{\partial t} = 0 \quad \text{Equation 2}$$

where $S_{cryo}$ is ice saturation, $\beta$ is thermal expansion, $K$ is thermal conductivity, and α is the compressibility of solid phase which is considered to be 1 when the solid is incompressible.

*Momentum balance* (Equation 3)

$$\nabla\cdot\left\{\sigma' - \alpha\left[(1-S_w)p_i + S_w p_w\right]\delta_{ij}\right\} + \left[(1-n)\rho_s + nS_w\rho_w + n(1-S_w)\rho_w\right]g = 0 \quad \text{Equation 3}$$

where $\sigma$ is stress and $\delta$ is Kronecker delta.

**Key constitutive equations**

**Thermal module**

Latent heat during phase change (Equation 4)

$$\dot{Q} = -l_{iw}\, n\rho_w\frac{\partial S_w}{\partial t} \quad \text{Equation 4}$$

where $l_{iw}$ is the latent heat to change phase of ice and water.

**Hydraulic module** (Equations 5, 6, and 7)

*Average pore pressure*

$$P = (1-S_w)p_i + S_w p_w \quad \text{Equation 5}$$

where $P$ is pore pressure.

*Pore-ice pressure*

$$p_i = S_f(T_f - T) + p_w \quad \text{Equation 6}$$

where subscripts *f* denotes freezing.

*Soil freezing characteristic curve (SFCC)*

$$\theta=\theta_r+\frac{\theta_s-\theta_r}{\left\{1+\left[S_f\left(T_f-T\right)/P\right]^n\right\}^m}S_{eff}=\frac{\theta-\theta_r}{\theta_s-\theta_r}=\left\{1+\left[S_f\left(T_f-T\right)/P\right]^n\right\}^{-m} \quad \text{Equation 7}$$

where subscripts $\theta$ denotes absolute temperature.

**Darcy's law** (Equation 8)

$$v_{ws}=\frac{k_{rw}k}{\mu_{rw}\mu}\left(-\nabla p_w+\rho_w g\right) \quad \text{Equation 8}$$

where $k_{rw}=\sqrt{S_{eff}}¿¿$, and $\mu_{rw}=1.5963\times10^{-2}\exp\left(\frac{509.53}{T-150}\right)$

**Mechanical module**

*Stress-strain relation (thermo-elasticity)* (Equation 9

$$\sigma'=D\cdot\varepsilon-K_d\beta_s\left(T-T_0\right)\delta_{ij} \quad \text{Equation 9}$$

Table 1. Physical parameters employed in the calculation

| Parameter | value |
|---|---|
| Specific heat of rock/solid phase | 710 [J/(kg*K)] |
| Specific heat of water | 4200 [J/(kg*K)] |
| Specific heat of ice | 2100 [J/(kg*K)] |
| Thermal conductivity of rock/solid phase | 5 [W/(m*K)] |
| Thermal conductivity heat of water | 0.565 [W/(m*K)] |
| Thermal conductivity heat of ice | 2.2 [W/(m*K)] |
| Density of rock/solid phase | 2300 [kg/m^3] |
| Density of water | 1000 [kg/m^3] |
| Density heat of ice | 900 [kg/m^3] |
| Hydraulic conductivity of backfill | 1e-7 [m/s] |
| Porosity of backfill | 0.42 [1] |
| Bulk modulus of backfill | 50 [MPa] |
| Poisson ratio of backfill | 0.2 [1] |

**Model Geometry and Setup**

As mentioned beforehand, several shafts will be bored to excavate the ore body, which will be then filled with backfill. The shafts are designed to have 5 m diameter and 400 m depth. Here in the first stage, an initial array of eight shafts is considered, where shafts 1 and 5 (Figure 2) are being studied for their thermal interaction, and the corresponding thermal behaviour is modelled and discussed. The backfill deposition is in eight sequences, and the time gap between each filling is 90 days. The deposition is completed in sequential numerical order (shafts 1–8). Given this timing, shaft 5 is backfilled on the 360$^{th}$ day after depositing backfill into shaft 1. To give a better insight into the influence of a later deposition sequence on a previously backfilled shaft, four cut points are set at 0.4 m to the left (cut point A) and right

(cut point B) boundary of shaft 1, respectively; the same is done for shaft 2 as cut point C and cut point D (Figure 3).

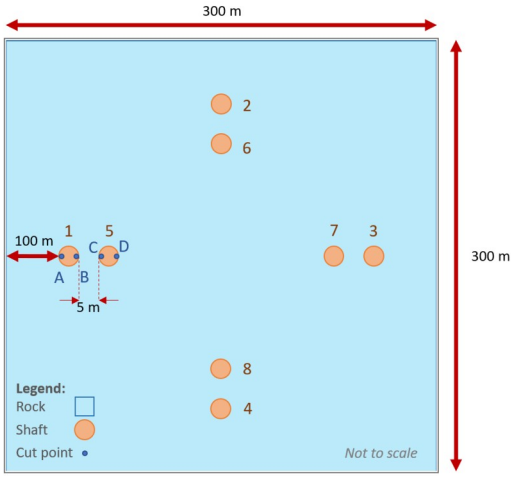


Figure 2. Configuration of plan-view of shaft array.

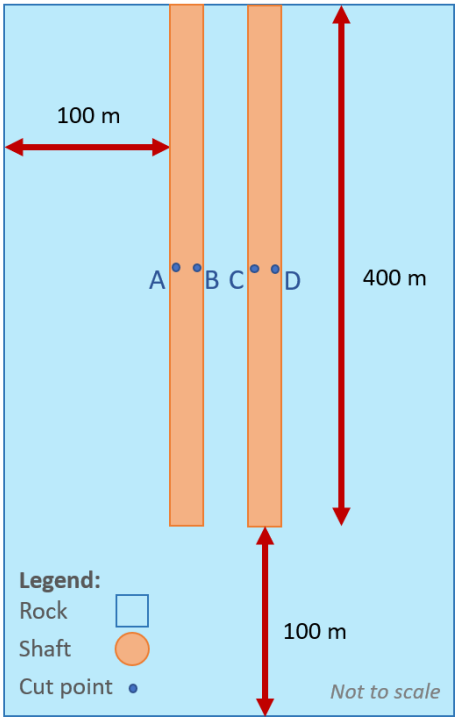


Figure 3. Configuration of the vertical-section view of shaft array

The initial temperature of the surrounding rock mass is set at -10 °C, based on the average soil temperature of the area. The initial temperature of the zero-cement backfill is 5 °C. Other operational parameters, as well as the temperature of the backfill, are given in Table 2. The boundary conditions applied to the model are shown in Table 3.

Table 2. Operational parameters employed in this study.

| Operational parameter | value |
|---|---|
| Rock mass temperature | –10 ℃ |
| Backfill temperature | 5 ℃ |
| Backfill diameter | 5 m |
| Shaft depth | 400 m |
| Distance between each backfill | 5 m |
| Time gap between each filling | 90 d |

Table 3. Details of initial and boundary conditions of the model.

| Physical field | Material IC/BC | Backfill | Rock |
|---|---|---|---|
| Thermal module | Initial condition | Initial backfill temperature | Rock temperature |
| | Boundary condition | Direct contact with rock mass | Rock temperature |
| Hydraulic module | Initial condition | Nil pore pressure | / |
| | Boundary condition | No flux in the periphery | / |
| Mechanical module | Initial condition | Nil displacement | / |
| | Boundary condition | Roller | / |

**Numerical Results and Discussion**

Based on the numerical results, the temperature evolution and ice saturation are the main parameters used in this section to illustrate the thermal behavior of the backfill during around 700 days. Figure 4 shows the temperature evolution cut points A and B, considering the fact that shaft 1 is filled with backfill in the beginning and then, after backfilling shafts 2–4 within 90 day gaps, shaft 5 is backfilled (~ 360 days after filling shaft 1) which affects cut point B.

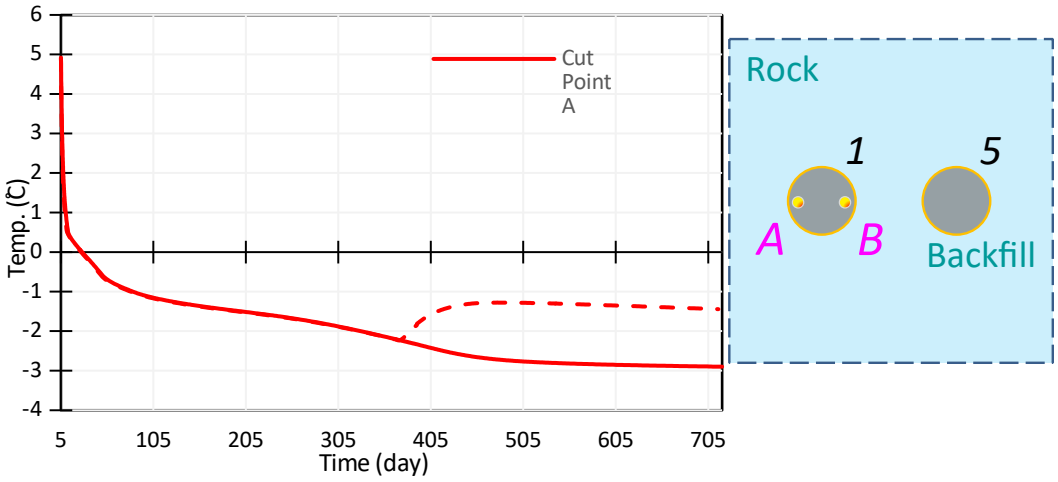


Figure 4. Temperature evolution of cut point A and B during the backfilling

As mentioned, after 360 days, shaft 5 is backfilled. This means that the higher temperature of backfill in shaft 5 likely affects cut point B (more than cut point A) because B is closer to shaft 5. The thermal behavior of cut points C and D are also indicated and inclued for comparison (Figure 5).

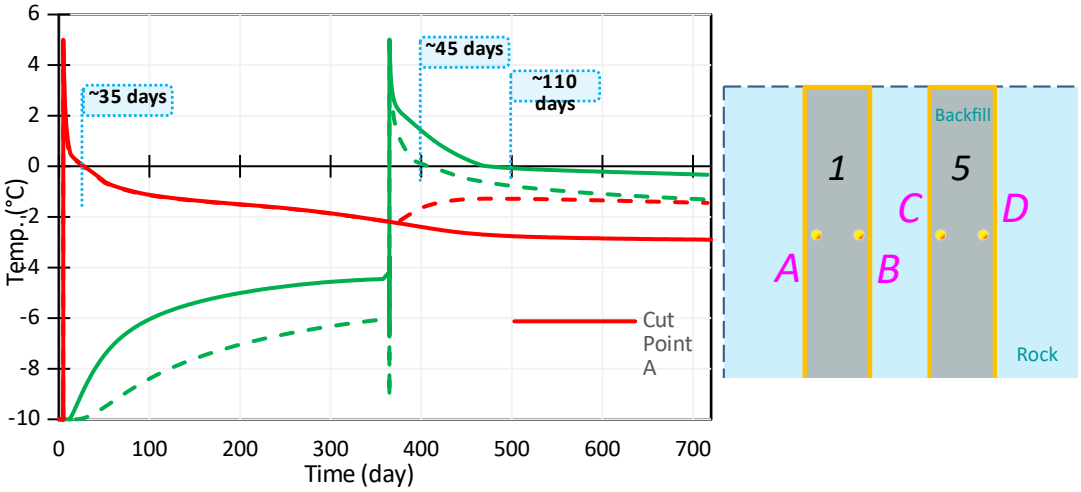


Figure 5. Temperature evolution in cut point A to D during backfilling and time duration each takes to show a temperature below 0 °C.

As can be seen in Figure 5, the temperatures of cut points B, C, and D are dramatically affected by backfilling shaft 5. Accordingly, cut points A and B take about 35 days to reach below 0˚C, while this time duration is ~ 110 days and ~ 45 days for cut points C and D, respectively. The longest freezing time belongs to C, which is almost twice, and three times higher than that of D and A. It is worth noting that cut points C and D indicate rock mass from day 0 to day 360, following which they indicate backfill.

Other than temperatures, ice saturation (Figure 6) is another parameter that can give better insight into the thermal behavior of backfill, as it shows the proportion of the water that has turned to ice. The heat that increases the temperature of cut point B decreases the ice saturation at the same time. The highest speed (tanα) of increasing in ice saturation is in cut points A and B (until day 360), followed by D, then C. Cut points A and B reach 0.5 ice saturation after ~ 200 days, while this time for cut point D would be > 350 days and for cut point C is estimated to be ~ 500 days.

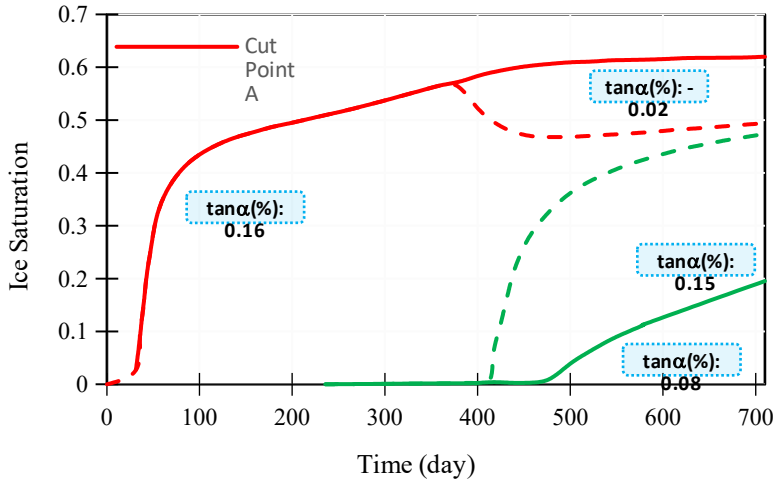


Figure 6. Ice saturation evolution at cut points A–D during backfilling.

Figure 7 displays the relationship between temperature and ice saturation. Plots of temperatures in cut points A–D show that although the temperature reaches below 0 ˚C, ice saturation is still very low at the moment just below 0 ˚C, as the water needs time to freeze.

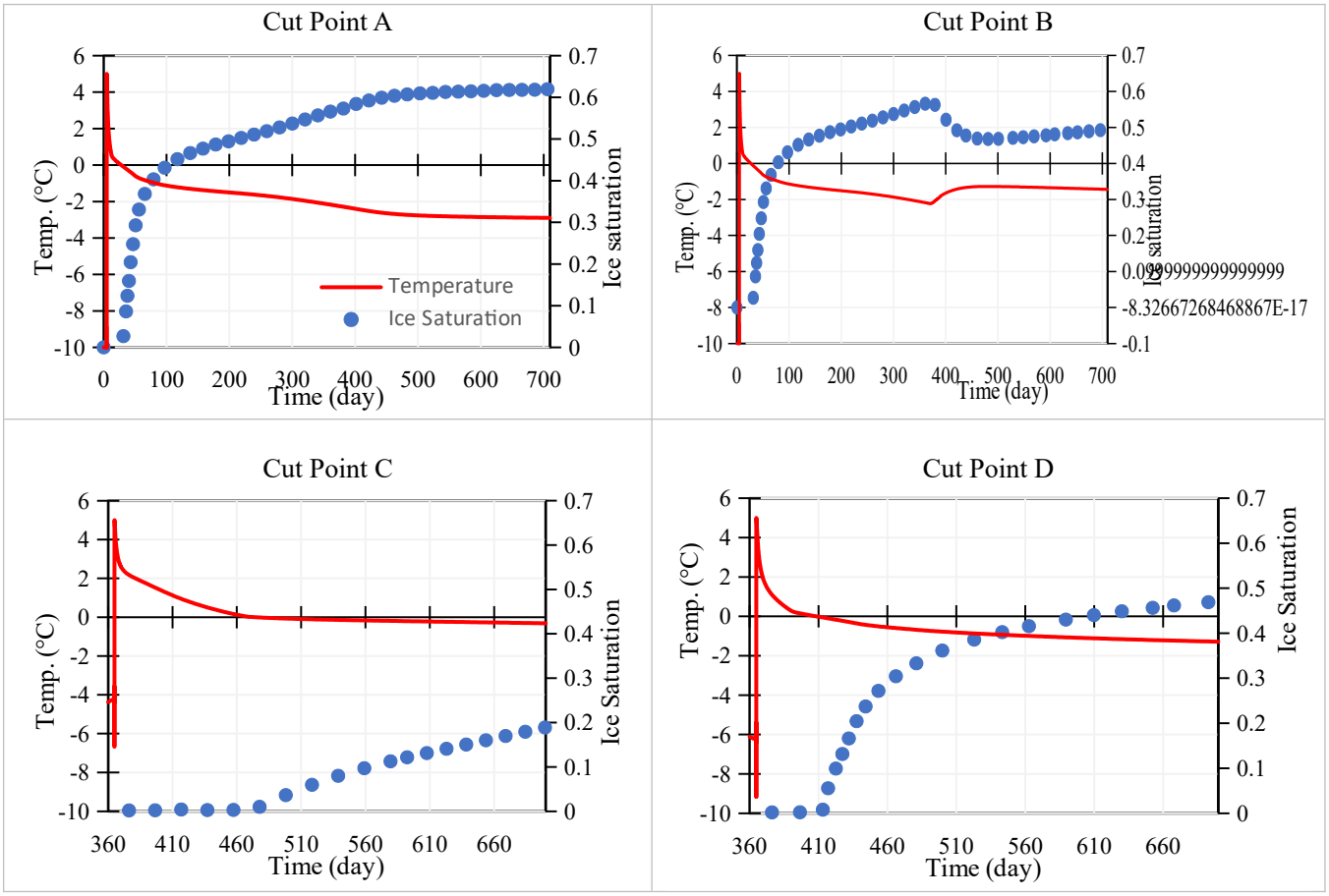


Figure 7. Temperature and ice saturation of each cut point over time.

**Conclusion**

We examined the thermal behavior of zero-cement backfill when surrounded with permafrost rock mass. Cement was omitted from the mixture of this backfill due to technical and practical difficulties, and water served as the binder in the backfill after freezing in the permafrost. A numerical model investigated the temperature and ice saturation of the backfill within a period of ~ 710 days, when two shafts were backfilled with a 360 day gap.

In shaft 1, when the backfill temperature was 5 ˚C and surrounded with -10 °C rock mass, freezing commenced after ~ 35 days. However, this did not mean that there would be a considerable amount of frozen backfill after 35 days according to ice saturation modeling. Indeed, ice saturation reached ~ 0.5 after around 200 days in cut point A, which meant that after 200 days, only about half of the water was frozen. This shows the significant importance of considering the ice saturation parameter alongside temperature evolution. Cut point B was apparently affected by the backfilling of shaft 2, although its temperature did not return to 0 °C or higher. Cut points C and D were also affected by the previous backfilling in shaft 1. Comparatively, the speed of cooling in cut point A was much higher than that of cut

point C, despite both being at the same position in their respective shafts. This can be attributed to cut point C being affected by the temperature of shaft 1, which was warmer than the surrounding rock mass.

The parameter ice saturation confirmed the results of temperature evolution. Any time that temperature drops, ice saturation surges and *vice versa*. The introduced ice saturation parameter gives a better understanding of how the freezing of backfill proceEds and is influenced by ambient conditions.
As this is an initial stage in numerical modeling of backfill thermal behavior, it should be done with additional attributes (different sequencing, shaft gaps, initial temperatures, etc.) in future.

**References**


Beya, F. K., Mbonimpa, M., Belem, T., Li, L., Marceau, U., Kalonji, P. K., Benzaazoua, M., & Ouellet, S. (2019). Mine backfilling in the permafrost, part I: Numerical prediction of thermal curing conditions within the cemented paste backfill matrix. *Minerals*, *9*(3). https://doi.org/10.3390/min9030165

Booshehrian, A., Wan, R., & Su, X. (2020). Hydraulic variations in permafrost due to open-pit mining and climate change: a case study in the Canadian Arctic. *Acta Geotechnica*, *15*(4), 883–905. https://doi.org/10.1007/s11440-019-00786-x

Bowes-Lyon, L.-M., Richards, J. P., & McGee, T. M. (2010). *Socio-Economic Impacts of the Nanisivik and Polaris Mines, Nunavut, Canada BT - Mining, Society, and a Sustainable World* (J. Richards (ed.); pp. 371–396). Springer Berlin Heidelberg. https://doi.org/10.1007/978-3-642-01103-0_13

Christ, M., Park, J.-B., & Hong, S.-S. (2010). Laboratory Observation of the Response of a Buried Pipeline to Freezing Rubber-Sand Backfill. *Journal of Materials in Civil Engineering*, *22*(9), 943–950. https://doi.org/10.1061/(asce)mt.1943-5533.0000090

Cluff, D. L., & Kazakidis, V. N. (2013). Opportunities and constraints of engineering frozen backfill for underground mining applications in permafrost. *ISCORD 2013: Planning for Sustainable Cold Regions - Proceedings of the 10th International Symposium on Cold Regions Development*, 175–190. https://doi.org/10.1061/9780784412978.018

DeBeers. (2022). *Chidliak Diamond Mine*.

Ed Struzik. (2023). In Rush for Key Metals, Canada Ushers Miners to Its Fragile North. *The Yale School of the Environment*. https://e360.yale.edu/features/canada-critical-minerals-mining

Fitzgerald, C., Grütter, H., Pell, J., & Pilotto, D. (2018). *2018 Technical Report: MINERAL RESOURCE UPDATE FOR THE CHIDLIAK PROJECT, BAFFIN ISLAND, NUNAVUT, CANADA Authors Qualified Persons Company*.

Gao, S. H., He, R. X., Jin, H. J., Huang, Y. D., Zhang, J. M., & Luo, D. L. (2017). Thermal recovery process of a backfilled open-pit in permafrost area at the Gulian strip coal mine in Northeast China. *JOURNAL OF MOUNTAIN SCIENCE*, *14*(11), 2212–2229. https://doi.org/10.1007/s11629-017-4439-3 WE - Science Citation Index Expanded (SCI-EXPANDED)

Ghoreishi-Madiseh, S. A., Hassani, F., Mohammadian, A., & Abbasy, F. (2011). Numerical modeling of thawing in frozen rocks of underground mines caused by backfilling. *INTERNATIONAL JOURNAL OF ROCK MECHANICS AND MINING SCIENCES*, *48*(7), 1068–1076. https://doi.org/10.1016/j.ijrmms.2011.09.002 WE - Science Citation Index Expanded (SCI-EXPANDED)

Hassani, F., & Archibald, J. (1998). *Mine backfill 1998*. Canadian Institute of Mining, Metallurgy and Petroleum.

He, R., Li, Y., Jin, H., Wang, H., Jin, X., Zhu, M., Li, X., Huang, Y., Jin, D., & Ma, F. (2022). Thermal Recovery of Backfilled Pit in the Gulianhe Strip Coalmine in the Hola Basin in Northern Da Xing'Anling Mountains, NE China. *Frontiers in Earth Science*, *10*(January), 1–17. https://doi.org/10.3389/feart.2022.806022

Hou, C., Zhu, W. C., Yan, B. X., Guan, K., & Du, J. F. (2020a). The effects of temperature and binder content on the behavior of frozen cemented tailings backfill at early ages. *CONSTRUCTION AND BUILDING MATERIALS*, *239*. https://doi.org/10.1016/j.conbuildmat.2019.117752 WE - Science Citation Index Expanded (SCI-EXPANDED)

Hou, C., Zhu, W., Yan, B., Guan, K., & Du, J. (2020b). The effects of temperature and binder content on the behavior of frozen cemented tailings backfill at early ages. *Construction and Building Materials*, *239*, 117752. https://doi.org/10.1016/j.conbuildmat.2019.117752

Jiang, H. Q., Fall, M., & Cui, L. (2017). Freezing behaviour of cemented paste backfill material in column experiments. *CONSTRUCTION AND BUILDING MATERIALS*, *147*, 837–846. https://doi.org/10.1016/j.conbuildmat.2017.05.002 WE - Science Citation Index Expanded (SCI-EXPANDED)

Lu, G. Da, Yang, X. G., Qi, S. C., Li, X. L., Ding, P. P., & Zhou, J. W. (2020). A generic framework for overpressure generation in sedimentary sequences under thermal perturbations. *Computers and Geotechnics*, *124*(April), 103636. https://doi.org/10.1016/j.compgeo.2020.103636

Pan, Z., Zhou, K., Wang, Y., Lin, Y., & Saleem, F. (2022). Comparative Analysis of Strength and Deformation Behavior of Cemented Tailings Backfill under Curing Temperature Effect. *Materials*, *15*(10). https://doi.org/10.3390/ma15103491

Seredkin, M., Zabolotsky, A., & Jeffress, G. (2016). In situ recovery, an alternative to conventional methods of mining: Exploration, resource estimation, environmental issues, project evaluation and economics. *Ore Geology Reviews*, *79*, 500–514.

Sheshpari, M. (2015). A review of underground mine backfilling methods with emphasis on cemented paste backfill. *Electronic Journal of Geotechnical Engineering*, *20*(13), 5183–5208.

Tao, J., Yang, X. G., Ding, P. P., Li, X. L., Zhou, J. W., & Lu, G. Da. (2022). A fully coupled thermo-hydro-mechanical-chemical model for cemented backfill application in geothermal conditions. *Engineering Geology*, *302*(March), 106643. https://doi.org/10.1016/j.enggeo.2022.106643

Tavanaei, F., Fadaei Kermani, M., Sasmito, A., Navarra, A., & Hassani, F. (2023). Application of Frozen backfill in a novel mining technique in the Arctic. *CIM 2023*.

Tilton, J. E. (2005). *Depletion and the long-run availability of mineral commodities*.

Xu, W. B., Han, M. R., & Li, P. (2020). Influence of freeze-thaw cycles on mechanical responses of cemented paste tailings in surface storage. *INTERNATIONAL JOURNAL OF MINING RECLAMATION AND ENVIRONMENT*, *34*(5), 326–342. https://doi.org/10.1080/17480930.2019.1595903 WE - Science Citation Index Expanded (SCI-EXPANDED)

Zhang, S. Y., Ren, F. Y., Guo, Z. B., Qiu, J. P., & Ding, H. X. (2020). Strength and deformation behavior of cemented foam backfill in sub-zero environment. *JOURNAL OF MATERIALS RESEARCH AND TECHNOLOGY-JMR&T*, *9*(4), 9219–9231. https://doi.org/10.1016/j.jmrt.2020.06.065 WE - Science Citation Index Expanded (SCI-EXPANDED)